A Journal of the Gesellschaft Deutscher Chemiker

Angewandte International Edition GDCh Chemie

www.angewandte.org

Accepted Article

Title: Unravelling the Enigma of Nonoxidative Conversion of Methane on Iron Single-Atom Catalysts

Authors: Jun Li, Yuan Liu, Jin-Cheng Liu, Teng-Hao Li, Zeng-Hui Duan, Tian-Yu Zhang, Min Yan, Wan-Lu Li, Hai Xiao, Yang-Gang Wang, and Chun-Ran Chang

To be cited as: *Angew. Chem. Int. Ed.* 10.1002/anie.202003908

Link to VoR: https://doi.org/10.1002/anie.202003908

WILEY-VCH

10.1002/anie.202003908

WILEY-VCH

COMMUNICATION

Unravelling the Enigma of Nonoxidative Conversion of Methane on Iron Single-Atom Catalysts

Yuan Liu,[a,d] Jin-Cheng Liu, [a] Teng-Hao Li,[b] Zeng-Hui Duan,[a] Tian-Yu Zhang,[c] Ming Yan,[b] Wan-Lu Li,[a] Hai Xiao,[a] Yang-Gang Wang,[d] Chun-Ran Chang,*[b] and Jun Li*[a,d]

Dedicated to Professor Xinhe Bao on the occasion of his 60th birthday

Abstract: The direct, nonoxidative conversion of methane on silica-confined single-atom iron catalyst ($Fe_1©SiO_2$) by Bao *et al*. (*Science*, 2014, *344*, 616) is a landmark discovery in catalysis science. However, the initially proposed gas-phase reaction mechanism is still open to discussion. Here, we report a surface reaction mechanism by comprehensive computational modelling and simulations. It is demonstrated that the activation of methane occurs at the single iron site, whereas the dissociated methyl disfavours desorption into gas phase under the reactive conditions. In contrast, the dissociated methyl prefers transferring to adjacent carbon sites of the active centre ($Fe_1©SiC_2$), followed by C−C coupling and hydrogen transfer to produce the main product (ethylene) via a key $-CH-CH_2$ intermediate. We find a quasi-Mars-van-Krevelen (quasi-MvK) surface reaction mechanism involving extracting and refilling the surface carbon atoms for the nonoxidative conversion of methane on $Fe_1©SiO_2$ and this new surface process is identified to be more plausible than the alternative gas-phase reaction mechanism.

With the increasing consumption of petroleum resources and the large-scale discovery of shale gas, natural gas hydrate and biogas, replacing oil by relatively abundant reserves such as natural gas to produce liquid fuels and basic chemicals has become the focus of research in academia and industry.[1-3] The conversion of methane can be realized either by *indirect routes* via synthesis gas (a mixture of CO and H_2)[4,5] or by *direct routes* such as the oxidative coupling of methane (OCM),[6,7] the selective oxidation of methane (SOM),[8-10] and the nonoxidative dehydroaromatization of methane (MDA).[11-15] Among them, the direct, nonoxidative route is the ideal one as it is more economic and environmentally friendly than the indirect routes with circumventing multiple reaction steps and the other oxidative direct routes often involving overoxidation. However, the direct, nonoxidative routes suffer from a significant challenge of methane activation because CH_4 has low electron affinity,[16] zero dipole moment[17] and high C-H bond energy (439 kJ/mol). Another disadvantage of nonoxidative routes is the severe thermodynamic constraints, which usually require high temperature and harsh conditions. Therefore, seeking unique catalysts for nonoxidative conversion of methane under relatively mild conditions is a long-term goal of the catalysis community.

In 2014, a breakthrough in nonoxidative conversion of methane was accomplished by Bao and colleagues,[18] who discovered that single iron sites embedded in a silica matrix enabled direct nonoxidative conversion of methane to ethylene and aromatics (MTOAH) at 1363 K. The conversion of methane reached at 48.1% and the selectivity to hydrocarbons exceeded 99% (ethylene selectivity > 48%). Of great importance is that no coke deposition and no catalyst deactivation were observed during a 60-hour test. MTOAH opens a new, atom-economical avenue for the direct transformation of methane.[19,20] The singly dispersed iron catalyst provides a novel example of utilizing heterogeneous single-atom catalysts (SACs) [21,22] for activating and transforming methane without producing awkward by-products. However, the mechanism of this promising new process remains elusive, despite the proposed gas-phase reaction mechanism based on VUV-SPI-MBMS analysis and preliminary theoretical calculations.[18] In the gas-phase mechanism, it is proposed that methane is firstly activated on the single-atom active centre ($Fe_1©SiC_2$) by C−H bond cleavage with dissociated methyl and H being adsorbed at Fe site and C site, respectively. Then, the methyl releases to gas phase to generate target ethylene and aromatics via gas-phase radical/molecule collision without the participation of catalyst surface. Although the gas-phase mechanism cannot be completely excluded, questions remain such as how the methyl releases to the gas phase upon strong adsorption at the surface and how is the selectivity of ethylene and aromatics controlled under gas-phase reaction mechanism.

[a] Dr. Y. Liu, Dr. J.-C. Liu, Z.-H. Duan, Dr. W.-L. Li, Assoc. Prof. Dr. H. Xiao, Prof. Dr. J. Li
Department of chemistry and Key Laboratory of Organic Optoelectronics & Molecular Engineering of Ministry of Education
Tsinghua University, Beijing 100084, China
E-mail: junli@tsinghua.edu.cn
[b] T. H. Li, M. Yan, Assoc. Prof. Dr. C. -R. Chang
School of Chemical Engineering and Technology, Shaanxi Key Laboratory of Energy Chemical Process Intensification
Xi'an Jiaotong University, Xi'an 710049, China
E-mail: changcr@mail.xjtu.edu.cn
[c] Dr. T. -Y. Zhang
Department of Chemistry and Biochemistry
Southern Illinois University Carbondale, IL 62901, USA
[d] Dr. Y. Liu, Assoc. Prof. Dr. Y. -G. Wang, Prof. Dr. J. Li
Department of Chemistry
Southern University of Science and Technology, Shenzhen 518055, China

Supporting information for this article is given via a link at the end of the document.

10.1002/anie.202003908

In this work, we have explored a variety of possible reaction mechanisms of MTOAH under realistic conditions by utilizing *ab initio* molecular dynamics (AIMD) simulations and static density functional theory (DFT) calculations in VASP software package.[23] We find that the activation of methane can occur on the surface of the catalyst. However, in contrast to the gas-phase reaction mechanism proposed in the literature,[18] the dissociated methyl prefers transferring to adjacent carbon site of the active centre rather than desorbing into the gas phase, which leads to a quasi-Mars-van-Krevelen (quasi-MvK) surface reaction mechanism that involves extracting and refilling surface C atoms coordinated to the Fe single-atom site.

Given the puzzles of gas-phase MTOAH reaction mechanism, we first used preliminary AIMD simulations to qualitatively explore various possible reaction mechanisms for this complicated reaction under reaction conditions. These simulations were helpful to providing clues for designing reasonable reaction mechanism that is further corroborated by static DFT calculations. The active centre $Fe_1©SiC_2$ (**Figure S1**) was built by coordinating Fe atom with two C atoms and one Si atom based on $Si©O_3$ unit of SiO_2(001) surface, which was identified by the experiment previously[18] and is supported by our recent computational study.[24] We first studied the C−H bond cleavage by methane colliding with the Fe site of $Fe_1©SiC_2$ with the initial velocity given by the mean kinetic energy of methane at 1363 K. It was found that methane could be activated by the Fe site (**Movie S1**), the selected snapshots and bond length variations are shown in **Figure 1**. There was a transitory adsorption state of methane on Fe atom at 0.15 ps (**Figure 1a**). Afterwards a transition state of the C−H bond activation of methane was found with the bond lengths of C1−H1 and C2−H1 being about 1.5 Å at 0.16 ps (**Figure 1b**), which indicates that single-atom Fe and neighbouring C sites play a synergistic role in activating the C−H bond. The C1−H1−C2−Fe four-centred transition state structure is reminiscent of that of methane activation on the ion-pair active centre of Co_3O_4 reported by Wang *et al.*[25]

We find that after methane activation the dissociated methyl formed an adsorption state on the top site of Fe rather than releasing to the gas phase as reported before.[18] The C1−Fe bond length was measured at ~2.0 Å, indicative of an effective C-Fe chemical bonding. Nevertheless, the methyl adsorption on Fe was only meta-stable and it continued to transfer to adjacent carbon site as the simulation proceeded at the high temperature. As shown in **Figure 1b**, at around 2.25 ps the bond length of C1−Fe dramatically increased and that of C1−C3 simultaneously reduced, indicating the transfer process of methyl from Fe site to C3 site. After 2.29 ps, the C1−C3 bond length remained at around 1.5 Å, suggesting the transfer of methyl and the formation of a $-C-CH_3$ intermediate. Whether methyl transfers or desorbs into gas phase is determinant to the subsequent transformation mechanism and thus demands in-depth analysis and validation. To this end, we performed 100 independent AIMD simulations from the adsorption state of methyl on Fe atom (**Int-1** in **Figure S2**). From these AIMD simulations, none of the methyls released to gas phase, 86% methyls diffused to adjacent unsaturated C site and 14% methyls kept still or diffused to Si site, as shown in **Figure S2**.

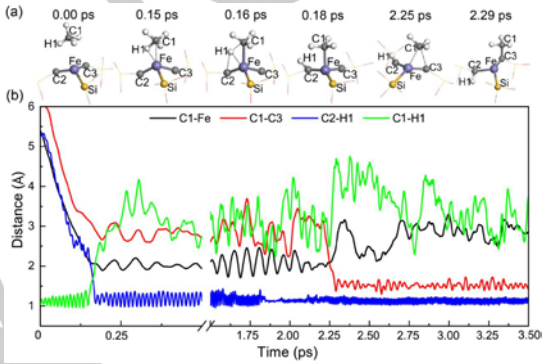

Figure 1. (a) Selected snapshots of AIMD trajectory for methane activation and methyl transfer at 1363 K, (b) The bond length variations versus simulation time in the AIMD trajectory.

Based on the AIMD simulations above, the whole pathways of methane converting to the main product (ethylene) on the catalyst surface were further investigated by using static DFT calculations. The whole reaction path network is shown in **Scheme S1**. **Figure 2** depicts the optimal reaction path from our calculations. For the first C−H bond cleavage of methane, overcoming a reaction barrier of 1.80 eV (**TS-1** in **Figure 2**) can generate CH_3 and H species. This step takes place at the Fe−C dual site of $Fe_1©SiC_2$, leading to CH_3 and H being anchored at Fe and C site, respectively. For comparison, the dissociation of CH_4 was also studied at the individual C site of $Fe_1©SiC_2$, which showed a much higher barrier (2.44 eV) than that on Fe−C dual site (**TS-1a** in **Figure S3**). Upon the crystal orbital Hamilton population (**COHP**) analysis of the C1−H1 bond in **TS-1** (**Figure 3a**), we found distinct bonding and antibonding states appear at −6.46 eV and −0.60 eV below the Fermi level in the electron occupied region, respectively. The linear combination of atomic orbitals (**LCAO**) of the bonding peak (**LCAO1** in **Figure 3a**) corresponds to a four-centred bond composed of 2*p* orbitals of C1/C2 atom, 1*s* orbital of H1 atom, and the 3*d* orbital of Fe atom. The chemical bonding analysis evidently

10.1002/anie.202003908
WILEY-VCH

COMMUNICATION

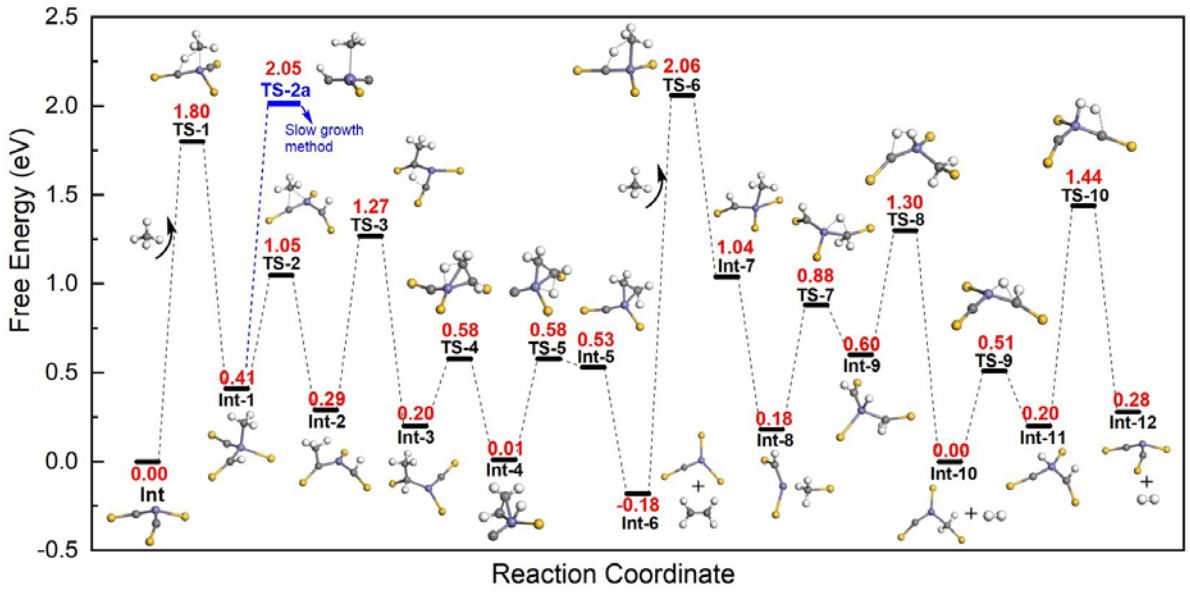

Figure 2. Free energy profiles at 1363 K and 1 atm with the corresponding structures of intermediates and transition states for methane activation and transformation on $Fe_1©SiC_2$ active centre. Methyl desorption barrier (**TS-2a**) was calculated by the slow growth method and the rest by static DFT method.

demonstrate the strong synergistic effect between Fe and C site in activating the first C-H bond of methane.

After the dissociative activation of methane, the methyl adsorbed on Fe site rapidly transfers to adjacent carbon sites as revealed by AIMD simulations. The methyl transfer barrier from **Int-1** was calculated as low as 0.64 eV (**TS-2** in **Figure 2**), which is some 1 eV lower than the methyl desorption barrier (**TS-2a** in **Figure 2**), further indicating the feasibility of the methyl transfer process. Alternatively, the adsorbed methyl may also further dissociate into CH_2 + H species, but the dissociation barrier was calculated as high as 1.92 eV (**TS-2e** in **Figure S3**), indicating such a pathway is difficult to occur compared with the competing transfer process. Such a high barrier for methyl dissociation may partially explain why the single-atom $Fe_1©SiC_2$ active centre can avoid coke deposition to some extent. The **COHP** analysis of **Int-1** and **TS-2** were also conducted to attain fundamental understanding on the reason why the path of methyl transferring is more favourable than the other two pathways. As shown in **Figure 3b**, although the delocalized π bonding among Fe−C1−C2−C3 (**LCAO3**) moiety makes the C1−Fe bond relatively stable in **Int-1** structure, the three-centred bonding between Fe and C1/C3 atoms in **LCAO4** (**Figure 3c**) could benefit the transfer of methyl from Fe atom to nearby C3 atom. The low barrier of 0.64 eV as well as the exothermic reaction energy of −0.12 eV shows the feasibility of methyl transfer from both kinetic and thermodynamic consideration.

Starting from the methyl-transferred structure **Int-2**, there are two pathways to form the final product ethylene. The first one is that another methane molecule comes in and is activated at the Fe−C active site of **Int-2**, as shown in Supplementary **Figure S4**. In this pathway, the activation of the second methane is the rate determining step with a barrier as high as 3.14 eV. In the other pathway based on the AIMD simulations (**Figure S5** and **Movie S2, S3**), the **Int-2** (−C−CH_3) first transforms to a −CH−CH_2 intermediate through two steps of hydrogen transfer (from **Int-2** to **Int-4** in **Figure 2**). Then, the −CH−CH_2 intermediate could further obtain a hydrogen atom from adjacent Fe site to generate an ethylene molecule (from **Int-4** to **Int-6**). Although these four elementary steps need to overcome several barriers (the highest of which is 0.98 eV), the overall reaction energy is exothermic by 0.47 eV, indicating this is a favourable pathway to occur.

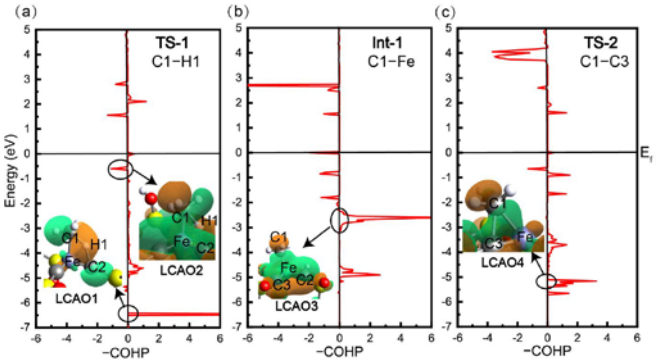

Figure 3. Calculated **COHP** of C1−H1 bond in **TS-1** structure, C1−Fe bond in **Int-1** structure and C1−C3 bond in **TS-2** structure. The orbitals correspond to the linear combination of atomic orbitals in the indicated electron occupied regions.

10.1002/anie.202003908

The active centre from **Int-6** can be recovered as soon as another methane is activated by Fe−C dual site of $Fe_1©Si_2C$. The barrier is as high as 2.24 eV (**TS-6**). Then, the methyl can easily transfer to silicon site with a downhill energy release of 0.86 eV to form the intermediate structure of **Int-8**. Similarly, the C−H bond in methyl group of **Int-8** can be activated by the Fe atom easily with a barrier of 0.70 eV (**TS-7**). The dissociated $-CH_2-$ and H atom are both bound to the Fe atom to form **Int-9**. Then, hydridic $H^{\delta-}$ from Fe site and protic $H^{\delta+}$ from C site combine together to generate a H_2 molecule with a barrier of 0.70 eV. At last, the remained two H atoms on carbon atom can also be released in the same way as hydrogen molecule to regenerate the original $Fe_1©SiC_2$ active centre. Overall, this pathway undergoes the activation of methane, the coupling of carbon species from methane and active centre, and the recovery of the active centre by gas-phase carbon recourse, which can be considered as a quasi-Mars-van-Krevelen (quasi-MvK) process that involves removing and refilling of carbon atom at the active site, as is sketched in **Scheme 1**.

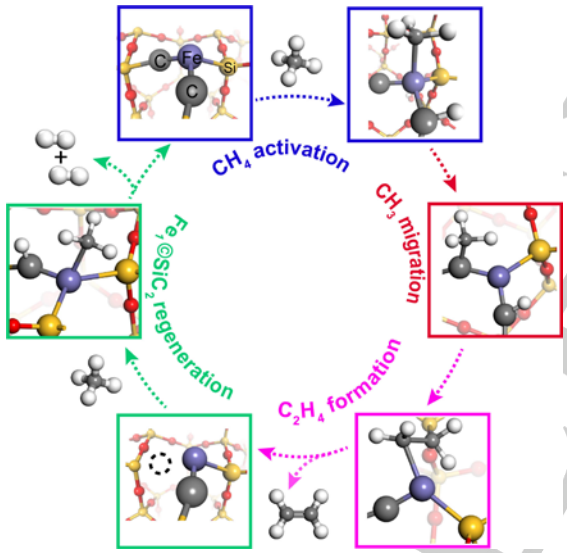

Scheme 1. Schematic illustration of quasi-Mars-van-Krevelen mechanism of methane conversion at the $Fe_1©SiC_2$ active centre.

As a whole, the generation of ethylene (from the starting point to **Int-6**) is a thermodynamically favourable process from the free energy profile (**Figure 2**). The barrier of methane activation (**TS-1**) is 1.80 eV, which corresponds to a rate constant of 6.78×10^6 s^{-1} at 1363 K based on the rate equation $k_{rate} = (k_BT/h)\times\exp(-\Delta G/RT)$, suggesting the feasibility of methane dissociation at high temperatures. After methane dissociation, the generation of ethylene via the surface mechanism only experiences a barrier of 0.98 eV (from **Int-1** to **Int-6**), which is about 1 eV lower than the barrier of gas-phase production of ethylene (**Scheme S2**), indicating the priority of surface reaction mechanism. The most difficult stage of the surface reaction mechanism is actually the regeneration of the active centre through the activation of a second methane and subsequent carbon insertion into the surface (from **Int-6** to **Int-12**), which possesses the highest activation barrier of 2.24 eV and is the rate determining step in the whole catalytic cycle; according to the energetic span model,[26] the rate constant is 1.63×10^5 s^{-1} at 1363 K. While for the gas-phase reaction mechanism, the regeneration of the active centre also needs to activate another methane and release a methyl radical into gas phase, the barrier of which is as high as 3.23 eV, as shown in **Figure S6**, which is 0.99 eV higher than that of our surface reaction mechanism. The ratio of rate constants between the surface reaction mechanism and the gas-phase reaction mechanism is about 4386:1, further indicating the favourite of the former. In this work, we focus on the production of the major product (ethylene). The heavier hydrocarbons, such as benzene and naphthalene identified in the experiment, might be formed upon oligomerization of dehydrogenated ethylene or further coupling of activated methyl with the C_2 species via the combined gas-phase and surface reaction mechanisms.

In summary, the reaction mechanisms of methane conversion on silica-confined iron SAC ($Fe_1©SiO_2$) are systematically studied by using combined AIMD simulations and static DFT calculation methods. Based on the preliminary AIMD simulations on the catalyst surface, the dissociated methyl from methane prefers transferring to adjacent carbon site at an $Fe_1©SiC_2$ active centre rather than desorbing into gas phase, which makes the surface reaction mechanism more likely than the gas-phase reaction mechanism. From the static DFT simulations on the surface catalytic cycle, the $-CH-CH_2$ species is identified to be a key surface intermediate to generate the final product ethylene. Overall, a new quasi-Mars-van-Krevelen surface reaction mechanism involving withdrawal and regenerating surface carbon atom during catalysis is revealed for the nonoxidative methane-to-ethylene conversion on $Fe_1©SiO_2$. Such a process involving carbon-atom recycling is relatively less observed, but is similar to the common Mars-van-Krevelen mechanism often acting in oxides, sulphides, chlorides, and hydrides. The involvement of both Fe and C at the active site indicates the importance of dual site synergetic interaction for complicated catalytic reaction.[27] These results provide a mechanistic understanding of nonoxidative conversion of methane on singly dispersed iron catalyst, which may stimulate design of more efficient or low temperature single-atom catalysts for the large-scale conversion of methane at nonoxidative conditions.

Acknowledgements

We thank Prof. Xinhe Bao, Prof. Xiulian Pan, and Dr. Liang Yu at Dalian Institute of Chemical Physics, Chinese Academy of Sciences for helpful discussion. This work was supported by National Natural Science Foundation of China (91645203, 21603170 and 21590792) and the China Postdoctoral Science Foundation (2018T111034 and 2018M630139). C. R. C. also gratefully acknowledges the Fundamental Research Funds for the Central Universities (xtr0218016 and cxtd2017004), the Rising Star Program in Science and Technology of Shaanxi Province (2020KJXX-079), the Shaanxi Creative Talents Promotion Plan-Technological Innovation Team (2019TD-039), and the support from K. C. Wong Education Foundation. The support of Guangdong Provincial Key Laboratory of Catalysis (No. 2020B121201002) is also acknowledged. The calculations were performed by using supercomputers at Tsinghua National Laboratory for Information Science and Technology, HPC Platform at Xi'an Jiaotong University, and the Supercomputer Center of Southern University of Science and Technology.

Keywords: methane • single-atom catalysis • computational simulation • reaction mechanism

[1] a) R. Horn, R. Schlogl, *Catal. Lett.* **2015**, *145*, 23-39; b) Z. J. Zhao, C. C. Chiu, J. L. Gong, *Chem. Sci.* **2015**, *6*, 4403-4425; c) A. I. Olivos-Suarez, A. Szecsenyi, E. J. M. Hensen, J. Ruiz-Martinez, E. A. Pidko, J. Gascon, *ACS Catal.* **2016**, *6*, 2965-2981; d) P. Schwach, X. L. Pan, X. H. Bao, *Chem. Rev.* **2017**, *117*, 8497-8520.

[2] a) R. H. Crabtree, *Chem. Rev.* **1995**, *95*, 2599-2599; b) H. Schwarz, *Angew. Chem., Int. Ed.* **2011**, *50*, 10096-10115; c) J. F. Weaver, C. Hakanoglu, A. Antony, A. Asthagiri, *Chem. Soc. Rev.* **2014**, *43*, 7536-7547; d) J. J. Spivey, G. Hutchings, *Chem. Soc. Rev.* **2014**, *43*, 792-803.

[3] a) J. H. Lunsford, *Catal. Today* **2000**, *63*, 165-174; b) E. McFarland, *Science* **2012**, *338*, 340-342; c) P. Tang, Q. J. Zhu, Z. X. Wu, D. Ma, *Energ. Environ. Sci.* **2014**, *7*, 2580-2591.

[4] a) G. Jones, J. G. Jakobsen, S. S. Shim, J. Kleis, M. P. Andersson, J. Rossmeisl, F. Abild-Pedersen, T. Bligaard, S. Helveg, B. Hinnemann, J. R. Rostrup-Nielsen, I. Chorkendorff, J. Sehested, J. K. Norskov, *J. Catal.* **2008**, *259*, 147-160; b) D. L. Li, Y. Nakagawa, K. Tomishige, *Appl. Catal. A-Gen.* **2011**, *408*, 1-24; c) D. Pakhare, J. Spivey, *Chem. Soc. Rev.* **2014**, *43*, 7813-7837.

[5] a) P. D. F. Vernon, M. L. H. Green, A. K. Cheetham, A. T. Ashcroft, *Catal. Today* **1992**, *13*, 417-426; b) A. P. E. York, T. C. Xiao, M. L. H. Green, *Top. Catal.* **2003**, *22*, 345-358.

[6] a) K. Kwapien, J. Paier, J. Sauer, M. Geske, U. Zavyalova, R. Horn, P. Schwach, A. Trunschke, R. Schlogl, *Angew. Chem., Int. Ed.* **2014**, *53*, 8774-8778; b) P. W. Wang, G. F. Zhao, Y. Wang, Y. Lu, *Sci. Adv.* **2017**, *3*, e1603180.

[7] a) G. E. Keller, M. M. Bhasin, *J. Catal.* **1982**, *73*, 9-19; b) T. Ito, J. X. Wang, C. H. Lin, J. H. Lunsford, *J. Am. Chem. Soc.* **1985**, *107*, 5062-5068; c) G. J. Hutchings, M. S. Scurrell, J. R. Woodhouse, *Chem. Soc. Rev.* **1989**, *18*, 251-283; d) J. H. Lunsford, *Angew. Chem., Int. Ed. Engl.* **1995**, *34*, 970-980.

[8] a) V. L. Sushkevich, D. Palagin, M. Ranocchiari, J. A. van Bokhoven, *Science* **2017**, *356*, 523-527; b) J. J. Xie, R. X. Jin, A. Li, Y. P. Bi, Q. S. Ruan, Y. C. Deng, Y. J. Zhang, S. Y. Yao, G. Sankar, D. Ma, J. W. Tang, *Nat. Catal.* **2018**, *1*, 889-896.

[9] a) S. Grundner, M. A. C. Markovits, G. Li, M. Tromp, E. A. Pidko, E. J. M. Hensen, A. Jentys, M. Sanchez-Sanchez, J. A. Lercher, *Nat. Commun.* **2015**, *6*, 7546; b) T. Ikuno, J. Zheng, A. Vjunov, M. Sanchez-Sanchez, M. A. Ortuno, D. R. Pahls, J. L. Fulton, D. M. Camaioni, Z. Y. Li, D. Ray, B. L. Mehdi, N. D. Browning, O. K. Farha, J. T. Hupp, C. J. Cramer, L. Gagliardi, J. A. Lercher, *J. Am. Chem. Soc.* **2017**, *139*, 10294-10301.

[10] a) M. H. Groothaert, P. J. Smeets, B. F. Sels, P. A. Jacobs, R. A. Schoonheydt, *J. Am. Chem. Soc.* **2005**, *127*, 1394-1395; b) J. S. Woertink, P. J. Smeets, M. H. Groothaert, M. A. Vance, B. F. Sels, R. A. Schoonheydt, E. I. Solomon, *Proc. Natl. Acad. Sci. U. S. A.* **2009**, *106*, 18908-18913; c) R. Palkovits, M. Antonietti, P. Kuhn, A. Thomas, F. Schuth, *Angew. Chemie., Int. Ed.* **2009**, *48*, 6909-6912.

[11] a) C. Y. Sun, G. Z. Fang, X. G. Guo, Y. L. Hu, S. Q. Ma, T. H. Yang, J. Han, H. Ma, D. L. Tan, X. H. Bao, *J. Energy Chem.* **2015**, *24*, 257-263; b) P. L. Tan, *J. Catal.* **2016**, *338*, 21-29; c) Y. Lai, G. Veser, *Catal. Sci. Technol.* **2016**, *6*, 5440-5452; d) K. D. Sun, D. M. Ginosar, T. He, Y. L. Zhang, M. H. Fan, R. P. Chen, *Ind. Eng. Chem. Res.* **2018**, *57*, 1768-1789.

[12] a) J. Yang, F. Deng, M. J. Zhang, Q. Luo, C. H. Ye, *J. Mol. Catal. A-Chem.* **2003**, *202*, 239-246; b) Z. R. Ismagilov, E. V. Matus, L. T. Tsikoza, *Energ. Environ. Sci.* **2008**, *1*, 526-541; c) J. Gao, Y. T. Zheng, J. M. Jehng, Y. D. Tang, I. E. Wachs, S. G. Podkolzin, *Science* **2015**, *348*, 686-690.

[13] a) D. Ma, Y. Y. Shu, X. W. Han, X. M. Liu, Y. D. Xu, X. H. Bao, *J. Phys. Chem. B* **2001**, *105*, 1786-1793; b) L. L. Su, D. Ma, X. M. Liu, Y. D. Xu, X. H. Bao, *Chinese J. Catal.* **2002**, *23*, 41-45; c) Y. D. Xu, X. H. Bao, L. W. Lin, *J. Catal.* **2003**, *216*, 386-395; d) L. L. Su, L. Liu, J. Q. Zhuang, H. X. Wang, Y. G. Li, W. J. Shen, Y. D. Xu, X. H. Bao, *Catal. Lett.* **2003**, *91*, 155-167; e) Y. Shu, R. Ohnishi, M. Ichikawa, *Appl. Catal. A-Gen.* **2003**, *252*, 315-329.

[14] a) C. L. Zhang, S. A. Li, Y. Yuan, W. X. Zhang, T. H. Wu, L. W. Lin, *Catal. Lett.* **1998**, *56*, 207-213; b) B. M. Weckhuysen, D. J. Wang, M. P. Rosynek, J. H. Lunsford, *J. Catal.* **1998**, *175*, 338-346; c) Y. D. Xu, L. W. Lin, *Appl. Catal. A-Gen.* **1999**, *188*, 53-67; d) S. T. Liu, L. Wang, R. Ohnishi, M. Ichikawa, *J. Catal.* **1999**, *181*, 175-188.

[15] a) L. S. Wang, L. X. Tao, M. S. Xie, G. F. Xu, J. S. Huang, Y. D. Xu, *Catal. Lett.* **1993**, *21*, 35-41; b) B. M. Weckhuysen, D. J. Wang, M. P. Rosynek, J. H. Lunsford, *Angew. Chem., Int. Ed. Engl.* **1997**, *36*, 2374-2376.

[16] a) C. G. Zhan, J. A. Nichols, D. A. Dixon, *J. Phys. Chem. A* **2003**, *107*, 4184-4195; b) N. J. Gunsalus, A. Koppaka, S. H. Park, S. M. Bischof, B. G. Hashiguchi, R. A. Periana, *Chem. Rev.* **2017**, *117*, 8521−8573.

[17] R. D. Amos, *Mol. Phys.* **1979**, *38*, 33-45.

[18] X. G. Guo, G. Z. Fang, G. Li, H. Ma, H. J. Fan, L. Yu, C. Ma, X. Wu, D. H. Deng, M. M. Wei, D. L. Tan, R. Si, S. Zhang, J. Q. Li, L. T. Sun, Z. C. Tang, X. L. Pan, X. H. Bao, *Science* **2014**, *344*, 616-619.

[19] a) A. T. Bell, *Sci. China Chem.* **2014**, *57*, 923-923; b) M. Sakbodin, Y. Q. Wu, S. C. Oh, E. D. Wachsman, D. X. Liu, *Angew. Chem., Int. Ed.* **2016**, *55*, 16149-16152; c) S. C. Oh, E. Schulman, J. Y. Zhang, J. F. Fan, Y. Pan, J. Q. Meng, D. X. Liu, *Angew. Chem., Int. Ed.* **2019**, *58*, 7083-7086.

[20] a) J. Q. Hao, P. Schwach, G. Z. Fang, X. G. Guo, H. L. Zhang, H. Shen, X. Huang, D. Eggart, X. L. Pan, X. H. Bao, *ACS Catal.* **2019**, *9*, 9045-9050; b) S. J. Han, S. W. Lee, H. W. Kim, S. K. Kim, Y. T. Kim, *ACS Catal.* **2019**, *9*, 7984-7997.

[21] a) B. Qiao, A. Wang, X. Yang, L. F. Allard, Z. Jiang, Y. Cui, J. Liu, J. Li, T. Zhang, *Nat. Chem.* **2011**, *3*, 634-641; b) X. F. Yang, A. Wang, B. Qiao, J. Li, J. Liu, T. Zhang, *Acc. Chem. Res.* **2013**, *46*, 1740-1748; c) A. Wang, J. Li, T. Zhang, *Nat. Rev. Chem.* **2018**, *2*, 65-81.

[22] a) J. C. Liu, Y. Tang, Y. G. Wang, T. Zhang, J. Li, *Natl. Sci. Rev.* **2018,** *5*, 638-641; b) J. X. Liang, Y. G. Wang, X. F. Yang, D. H. Xing, A. Wang, T. Zhang, J. Li, *Encyclopedia Inorg. Bioinorg. Chem.* **2017**, pp.1-11. DOI: 10.1002/9781119951438.eibc2448; c) J.-C. Liu, H. Xiao, J. Li, *J. Am. Chem. Soc.* **2020**, *142*, 3375-3383.

10.1002/anie.202003908

[23] a) G. Kresse, J. Furthmuller, *Comp. Mater. Sci.* **1996**, *6*, 15-50; b) G. Kresse, J. Furthmuller, *Phys. Rev. B* **1996**, *54*, 11169-11186.
[24] T. H. Li, M. Yan, Y. Liu, Z. Q. Huang, C. R. Chang, J. Li, *J. Phys. Chem. C* **2020**, *124*, 13656-13663.
[25] Y. G. Wang, X. F. Yang, L. H. Hu, Y. D. Li, J. Li, *Chinese J. Catal.* **2014**, *35*, 462-467.
[26] S. Kozuch, S. Shaik, *Acc. Chem. Res.* **2011**, *44*, 101-110.
[27] J. X. Liang, J. Lin, J. Y. Liu, X. D. Wang, T. Zhang, J. Li, *Angew. Chem., Int. Ed.* **2020**, *59*, 2-10.

10.1002/anie.202003908

WILEY-VCH

COMMUNICATION

Entry for the Table of Contents

COMMUNICATION

A *quasi*-Mars-van-Krevelen new surface reaction mechanism involving withdrawal and regenerating surface carbon atom during nonoxidative catalytic conversion of methane on $Fe_1©SiC_2$ is found.

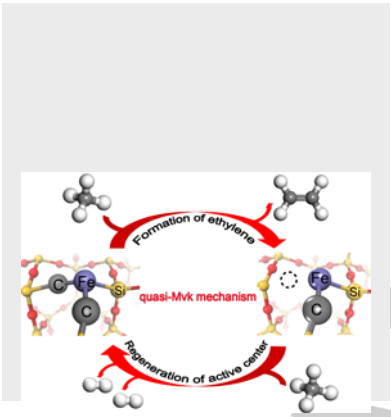

Yuan Liu, Jin-Cheng Liu, Teng-Hao Li, Zeng-Hui Duan, Tian-Yu Zhang, Ming Yan, Wan-Lu Li, Hai Xiao, Yang-Gang Wang, Chun-Ran Chang, and Jun Li**

Page No. – Page No.

Unravelling the Enigma of Nonoxidative Conversion of Methane on Iron Single-Atom Catalysts